JOURNAL OF MAGNETIC RESONANCE **126,** 242–247 (1997)
ARTICLE NO. MN971155

ESR and TPD Investigations of the Adsorption of Di-*tert*-butyl Nitroxide on Au(111) and NiO(111). Evidence for Long-Range Interactions

U. J. Katter, T. Risse,* H. Schlienz, M. Beckendorf, T. Klüner,* H. Hamann,* and H.-J. Freund*

Lehrstuhl für Physikalische Chemie I, Ruhr-Universität Bochum, 44780 Bochum, Germany

Received December 17, 1996; revised February 21, 1997

Electron spin resonance and temperature-programmed desorption spectra of thin layers of DTBN (di-*tert*-butyl nitroxide) adsorbed on Au(111) and NiO(111)/Au(111) surfaces have been measured. The temperature-programmed desorption data show a weak chemisorption of the DTBN molecules in the monolayer on both surfaces. On Au(111) as well as on NiO(111)/Au(111), the ESR signal from monolayer coverages is totally suppressed. This suppression continues into the multilayer regime on both substrates. Disturbances of the substrate/adsorbate interface have a strong influence on the range of the signal suppression. Possible reasons for this behavior are discussed.

INTRODUCTION

ESR spectroscopy is a method well suited to the study of molecular motions (*1*). Because of its high sensitivity, it is now possible to investigate adsorbates on single crystal surfaces (*2–4*). A disadvantage of the method is that only paramagnetic molecules can be used as adsorbates. The study of lineshape changes in the ESR spectrum caused by molecular motion, on the other hand, is an interesting field, because a broad range of motional frequencies is covered and it is possible to decide between various theoretical models proposed for molecular motion (*5*). The spectrum may also contain more information about the interaction between adsorbate and substrate and between the adsorbed molecules themselves.

But there is a second limitation to the applicability of the ESR technique in surface science: First experiments have been concerned with the adsorption of molecules on metal surfaces but failed in obtaining ESR spectra from monolayers of the adsorbed radicals (*6, 7*). This is caused by an interaction between the unpaired electron of the paramagnetic molecule and the conduction electrons of the metal, which is expected to be short ranged and to influence only the first layer of the adsorbed molecules. However, Barkley *et al.* (*8*) reported that up to 62 layers of adsorbed nitroxide molecules can be affected. In this paper we corroborate this result for the system di-*tert*-butyl nitroxide (DTBN)/Au(111) using a different experimental setup.

If, instead of a metal, an oxide is used as substrate, ESR signals of molecular monolayers may well be observed. Examples are DTBN, NO_2, and self-assembled fatty acid films on a thin epitaxial Al_2O_3 layer (*2–4*). It appears, however, that a magnetic oxide as substrate may cause complications: For the system DTBN adsorbed on an epitaxially grown NiO(111) film, we report here on a strong suppression effect which is surprising in view of the poor conductance of NiO. We invoke magnetic coupling to explain the phenomenon.

EXPERIMENTAL

The ESR measurements were performed in a specially designed UHV ESR chamber which has been described in detail previously (*7*), as have the special sample design and the use of a liquid helium cryostat, which allows cooling the crystal to 40 K. A Bruker B-ER 420 ESR spectrometer has been used with some modifications for the connection to the UHV chamber. The UHV chamber is equipped with a quadrupole mass spectrometer that allows the recording of temperature-programmed desorption (TPD) spectra and with a combined LEED/Auger unit for substrate characterization. The base pressure is less than 1×10^{-10} mbar.

The Au(111) single crystal (orientational deviation $<1\%$) was cleaned by sputter and heating cycles until no impurities could be detected with Auger spectroscopy and the LEED pattern showed the sharp and hexagonally arranged reflections of the (111) surface. The $22 \cdot \sqrt{3}$ reconstruction described in the literature (*9*), however, could be seen only weakly. To prepare an epitaxial NiO(111) layer, Ni of high purity (99.98%) was evaporated in 1×10^{-6} mbar O_2 on the well-prepared Au(111) surface according to a recipe by Marre and Neddermeyer (*10*). The evaporation was continued well above the point when the Au signal disappears in the Auger spectrum and the substrate crystal has been completely covered with a NiO film. The broad reflections of the LEED pattern indicate a higher density of

* New address: Fritz-Haber-Institut der Max-Planck-Gesellschaft, Faradayweg 4-6, 14195 Berlin, Germany.

1090-7807/97 $25.00

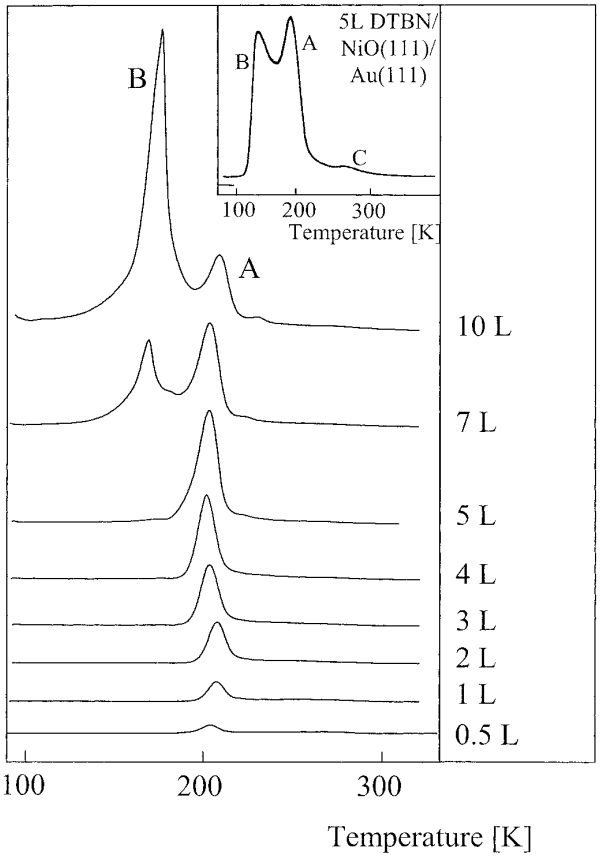

FIG. 1. Thermal-programmed desorption spectra of DTBN/Au(111). The intensity of the fragment with $m/e = 41$ is shown. The features are discussed in the text. The inset shows a TPD spectrum of DTBN/NiO(111)/Au(111) for comparison.

defects as compared with the Au(111) surface. This is in line with STM observations (*11*).

DTBN (Lancaster) was used as commercially purchased but after careful degassing. It was stored in glass bottles attached to a dosing valve, which led into the UHV chamber. Before dosing, the bottle was warmed to approximately 50°C to increase the vapor pressure. The chamber was then flooded with DTBN. The exposures are given in langmuir units; L ≡ Torr · s.

The program for simulating and fitting the experimental spectra was written by Beckendorf (*12*) and is based partly on a program package developed by Freed and co-workers (*13*). Axial symmetry of g and A tensors ($g_{xx} = g_{yy}$, $A_{xx} = A_{yy}$) (*14*) and spatial random distribution of molecular orientations have been assumed for the simulations. Lorentzian lineshapes have been used. Linewidths are given as full widths at half-maximum.

EXPERIMENTAL RESULTS

Temperature-Programmed Desorption

Figure 1 shows TPD spectra after dosing between 0.5 and 10 L DTBN to the Au(111) surface at 90 K. Since the quadrupole mass filter used has a low transmission for high masses, it was not possible to detect the molecular ion with $m/e = 144$ in the monolayer regime. The signals of highest intensity in the cracking pattern of DTBN (using an ionization energy of 70 eV) with $m/e = 39$ ($C_3H_3^+$, not shown here) and 41 (CH_3CN^+) can be used instead to follow the desorption from the surface as multimass data revealed. A discussion of the cracking pattern has been given by Kostyanovskii and Khafizov (*15*).

The TPD spectra in Fig. 1 show two features, marked A and B. Peak A at a desorption temperature of about 205 K is attributed to the monolayer and saturates at a dose of about 5 L DTBN. From the Redhead formula for first-order desorption (*16*), an activation energy of 53 kJ/mol is estimated. Peak B at a desorption temperature of 170 K appears only after exposures greater than 5 L and increases with increasing DTBN dose. No saturation of this desorption state could be obtained. It is therefore due to the desorption of the DTBN multilayer. The desorption energy is estimated to be 44 kJ/mol.

The inset in Fig. 1 shows a TPD spectrum of 5 L DTBN on NiO(111)/Au(111) for comparison. This system reveals the same mono-/multilayer behavior as that discussed earlier. The monolayer, peak A, desorbs at a temperature of about 200 K, from which the desorption energy of 51 kJ/mol is estimated. Therefore the interaction of the DTBN molecules on this oxide surface is comparable to that with Au(111). Additionally, a small feature (C) at a desorption temperature of 270 K has been observed. It is attributed to a contamination of the surface with hydroxyl groups, which are known to be formed on NiO(111) grown on Ni(111) (*17*). The desorption energy of 70 kJ/mol is about 19 kJ/mol higher than that of the monolayer (A). This larger interaction energy is compatible with the additional energy of a DTBN–OH bond, which has been estimated from a calculation of the binding energy of a DTBN–H_2O complex (on the 6-31G* ROHF plane) (*18*) to be 15.4 kJ/mol.

ESR

Au(111). No ESR signal could be detected after dosages of 5, 7.5, 10, or 50 L DTBN to the clean Au(111) surface at 40 K. These dosages correspond to increasing coverages leading to multilayer adsorption of DTBN determined from the clear mono-/multilayer behavior of the TPD data. The first spectrum was obtained from a dose of 100 L DTBN. This corresponds formally to 20 layers, if the growth mode is of layer-by-layer type. The ESR spectrum is shown at the top of Fig. 2. If the substrate temperature was held at 80 K while 100 L DTBN is adsorbed, no ESR spectrum could be detected, indicating that indeed the growth mode of the DTBN aggregates plays an important role. In fact this observation is compatible with three-dimensional Volmer–Weber growth at low temperature.

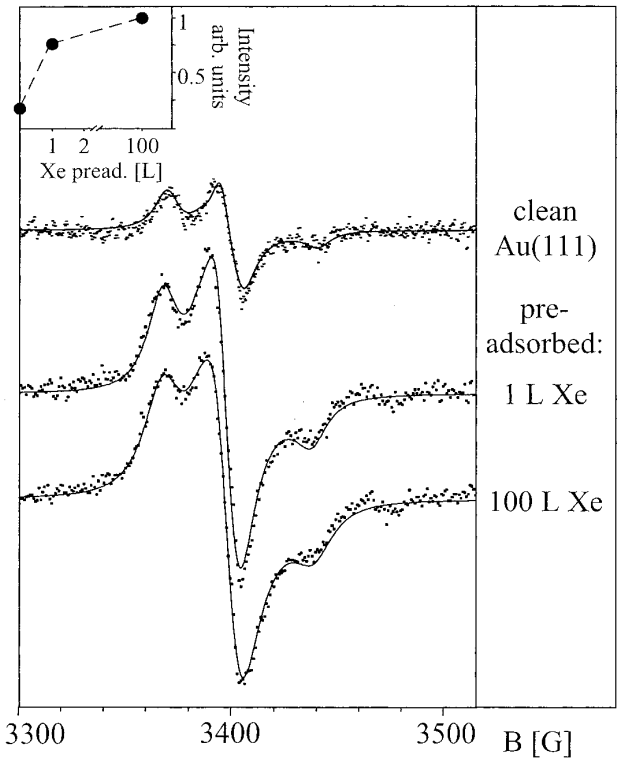

FIG. 2. ESR spectra of 100 L DTBN/Au(111). The first spectrum is measured after adsorption on the clean surface, and the second and third spectrum after preadsorption of 1 and 100 L xenon, respectively. The inset shows the course of the integral intensities.

To weaken the interaction between substrate and adsorbate (*19*), 1 L xenon, which corresponds to a monolayer, has been preadsorbed on the clean Au(111) surface followed by a dose of 100 L DTBN. Afterward the second spectrum in Fig. 2 was measured. The intensity is now considerably higher than that in the upper trace. To obtain complete decoupling between substrate and adsorbate, a xenon multilayer is formed via dosing 100 L Xe, followed by a dose of 100 L DTBN. (The ability to adsorb xenon multilayers at a substrate temperature of 40 K has previously been checked with TPD spectroscopy.) The spectrum at the bottom of Fig. 2 shows the corresponding ESR signal. As the inset in Fig. 2 shows, the signal intensity has increased again to a maximum value (to which the other intensities have been normalized). From the ESR intensities it can be estimated that on the clean Au surface about 83% (formally 17 of 20 layers) of the DTBN molecules are influenced by the interaction with the substrate such that their ESR signal is suppressed. The intensity missing in the second spectrum can be attributed to various causes: for example, the interaction between substrate and paramagnetic adsorbate can penetrate to a certain degree through one xenon layer, or the existence of areas of uncovered substrate allowing direct contact between the Au surface and some of the DTBN molecules.

The spectra have been simulated and the parameters obtained from the simulations are given in Table 1: The absolute g values have not been referenced to a standard and are thus not significant, but their splitting Δg, the difference between g_{zz} and $g_{xx} = g_{yy}$, is consistent with that reported previously for DTBN adsorbed on other surfaces (*2, 20*). In contrast, the A-tensor components are known to depend strongly on the chemical surroundings of the molecule (*21*). Their values presented here are of some interest, since they should be typical for DTBN in a DTBN matrix. In solid DTBN, the hyperfine structure is completely averaged out by the exchange interaction. In the present case, the DTBN aggregates are too small to show intense exchange interaction, although an exchange rate must be included in the parameters of the simulation. This rate and the evolution of the linewidths will give some information about the nature of the substrate/adsorbate interaction. Both values increase with increasing fraction of ESR-active molecules.

NiO(111)/Au(111). On the clean NiO(111) surface, no ESR signal could be detected after dosages as large as 100 or 200 L DTBN. After the crystal was exposed to a dose of 400 L DTBN (formally 80 layers), the uppermost spectrum in Fig. 3 was measured. A comparison of the integral intensity shows that only 12% of the adsorbed material is ESR active. Therefore the effect of suppressing the ESR spectra on this substrate is even more long range than that on Au(111) under similar adsorption conditions. The parameters for simulating the spectrum are also presented in Table 1, but show no significant differences from those found on Au(111).

The DTBN multilayer was slowly warmed and the changes in the ESR spectra are shown in Fig. 3. (The spectra are normalized to the same peak-to-peak amplitude to show the effect more clearly.) There is an increasing loss of hyperfine structure with increasing temperature. At 163 K the spectrum consists of only a single line. This irreversible change can be simulated by increasing the exchange rate while keeping all other parameters nearly constant. The heating procedure activates motional degrees of freedom such as molecular rotations or translations in the multilayers which lead to a more ordered structure with more pronounced orbital overlap. It is remarkable that the ESR intensity shows no variation from a Curie behavior. This means that there is no conversion from an ESR-inactive to an ESR-active state or vice versa as observed on Al_2O_3 (*2*). Above 163 K the signal vanishes as the multilayer desorbs. The remaining monolayer could not be detected via ESR.

As on Au(111), the ESR signal can be enhanced by preadsorbing xenon on the NiO(111) surface. In contrast, however, to the experiments on Au(111), the enhancement from dosing with the same amount of xenon is less pronounced. This may be an effect of a different growth mode of the xenon layers (e.g., formation of three-dimensional islands

TABLE 1
Fitting Parameters for the Spectra Shown in Figs. 2 and 3

	$g_{xx} = g_{yy}$	g_{zz}	Δg	$A_{xx} = A_{yy}$	A_{zz}	ΔB [G]	ν_{ex} [Hz]	I %
100 L DTBN	2.0060	2.0005	0.0055	6.7	35.7	11.0	5.1×10^7	17
/1 L Xe	2.0071	2.0023	0.0048	7.2	35.2	12.0	8.9×10^7	76
/100 L Xe	2.0060	2.0011	0.0049	7.6	35.8	16.0	9.7×10^7	100
400 L DTBN/NiO(111)	2.0062	2.0010	0.0052	7.5	35.5	12.3	4.1×10^7	50

versus layer-by-layer growth). Contamination of the NiO(111) surface with residual gas (e.g., exposing the cold surface to the chamber atmosphere for two hours before DTBN adsorption) also reduces the number of affected DTBN layers.

DISCUSSION

The suppression of the ESR signals of paramagnetic molecules on metal surfaces is known to be caused by an exchange interaction between the unpaired electron of the paramagnetic molecule and the conduction electrons of the metal (*6, 7*). This interaction leads to a decrease in the lifetime of the unpaired electron which causes a massive broadening of the ESR lines, leaving them undetectable. The degree of broadening has been estimated with the Anderson Hamiltonian originally used to describe exchange of $3d$ elements embedded in metals (*22*). This approach, however, cannot be used to explain the range of the interaction found in this study and also by Barkley *et al.* (*8*), who adsorbed different nitroxide molecules on metal films evaporated on the inner walls of an UHV cavity. The amount of ESR-nonactive nitroxide molecules in Barkley's data ranges formally from 2 to 62 layers depending on the type of nitroxide and metal substrate. The theoretical problem is to explain how molecules far away from the surface can interact with the conduction electrons of the metal substrate. Eigler and Schultz (*23*) have already shown that the adsorbates on a metal surface influence the distribution of the conduction electrons: In their conduction-electron spin-resonance experiments they found that adsorption of xenon and krypton atoms on a lithium surface leads to a pileup of conduction-electron density above the surface. Additional calculations showed that conduction-electron density has been mixed into orbitals of the rare gas atoms. In the case of nitroxide molecules, the half-filled orbitals, responsible for their paramagnetism, may even serve as a better carrier for conduction-electron density or for the interaction itself. The important point is the growth mode of the DTBN molecules on the surface.

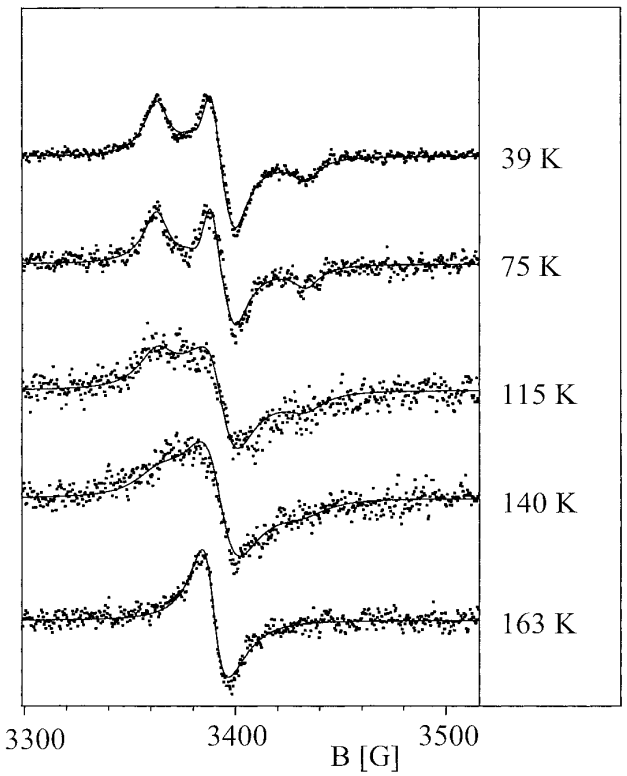

FIG. 3. ESR spectra of 400 L DTBN/NiO(111)/Au(111) as a function of temperature. The spectra are discussed in the text.

We believe that the molecules arrange in small, ordered aggregates with effective orbital overlap inside. The exchange rate ν_{ex} then depends on the size of these aggregates, if exchange between the aggregates can be neglected. Those aggregates forming on the surface initially have direct contact to the metal substrate and the conduction electrons may interact with the molecules over a long range via ''cluster orbitals.'' This type of interaction should be restricted to the molecules forming the first layer of clusters, so that the propagation of the interaction is prohibited at the grain boundaries. Figure 4 shows a schematic illustration. This model also explains why a satisfactory simulation of the ESR spectra can be carried out with a simple parameter set instead of a superposition of several spectra with decreasing linewidths, which would correspond to an interaction decaying layer-by-layer.

This interpretation is also in line with the variation of the linewidth and exchange rate in the spectra shown in Fig. 2. The ESR-active molecules belonging to the uppermost

spectrum are situated in small clusters attached to the first layer of inactive clusters, and the exchange rate is low. After preadsorption of xenon, the number of ESR-active molecules increases while the cluster size is larger and more uniformly distributed. The increase in linewidth, which is probably dominated by dipolar interactions, shows that the inactive molecules do not contribute to the static dipolar fields. This is in accord with a rapid spin-exchange mechanism, which would average out the dipolar fields.

The suppression of the ESR spectra of DTBN on NiO(111) must be of different origin, because no conduction electrons are present on this oxide surface. We believe that the effect is connected with the strong antiferromagnetism of the NiO substrate (T_{Neel} = 520 K) (*24*). ESR studies concerning the adsorption of paramagnetic molecules on antiferromagnetic substrates are in fact conspicuously rare. Matsunaga and McDowell (*25*), for example, reported, for the system DPPH (α,α-diphenyl-β-picrylhydrazyl) adsorbed on polycrystalline NiO, a decrease of 80% of the ESR intensity compared to that found on a nonmagnetic KCl substrate. The reason for the loss of intensity can be an interaction between the unpaired spins of the Ni ions, which are strongly coupled by superexchange interactions, and the spins located at the adsorbed molecules. If a coupling to the substrate spins becomes the dominating interaction for the adsorbate spins, the Zeeman effect is canceled and the ESR spectra are suppressed. In contrast to the effect discussed for DTBN on Au(111), the ESR lines would not be broadened by a lifetime effect; they are completely absent. A different mechanism, which could bridge cluster boundaries (see discussion above), would also account for the longer range.

This explanation is supported by the fact that nitroxide molecules show antiferromagnetic interactions at very low temperatures in the solid phase (*26–28*), but the retention of ESR inactivity up to the desorption temperature of 170 K (see Fig. 3) appears questionable within this model. But there exist parallels between the present results and those of Borchers *et al.* (*29*), who examined the magnetic properties of CoO/NiO sandwich structures with neutron diffraction. The spins in the CoO layers showed antiferromagnetic ordering in these layered structures up to 80 K above the bulk Neel temperature (291 K). This behavior was interpreted to be caused by an interaction with the strong antiferromagnetic NiO layers. A corresponding effect may be responsible for the absence of an ESR signal of DTBN adsorbed on NiO(111).

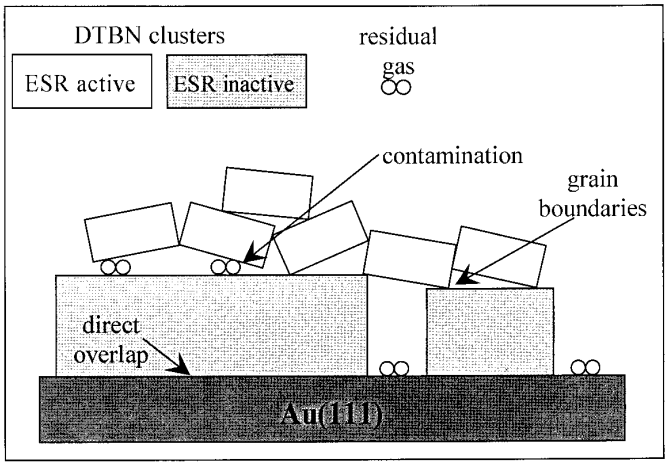

FIG. 4. Illustration of the supposed growth mode for the DTBN clusters on the Au(111) surface responsible for the range of the observed adsorbate/substrate interaction.

SUMMARY

The suppression of ESR spectra of DTBN multilayers adsorbed on Au(111) is discussed on the basis of spin exchange between the unpaired electron of the molecule and the conduction electrons of the metal. The long range of the interaction can be mediated by the overlap of the half-filled molecular orbitals forming ''cluster orbitals.'' On NiO(111) a magnetic coupling of the adsorbate spins to the strong antiferromagnetic substrate can be responsible for the suppression observed.

ACKNOWLEDGMENTS

The authors are grateful to the Deutsche Forschungsgemeinschaft, the Ministerium für Wissenschaft und Forschung des Landes Nordrhein-Westfalen, the Bundesministerium für Bildung und Forschung, and the Fonds der Chemischen Industrie for financial support. T. Risse and T. Klüner thank the Studienstiftung des Deutschen Volkes for financial support.

REFERENCES

1. J. H. Freed, *in* ''Spin Labeling: Theory and Applications'' (L. J. Berliner, Ed.), Academic Press, New York/San Francisco/London, 1976.
2. U. J. Katter, T. Hill, T. Risse, H. Schlienz, M. Beckendorf, T. Klüner, H. Hamann, and H.-J. Freund, *J. Phys. Chem.* B, **101,** 552 (1997).
3. H. Schlienz, M. Beckendorf, U. J. Katter, T. Risse, and H.-J. Freund, *Phys. Rev. Lett.* **74,** 761 (1995).
4. T. Risse, M. Beckendorf, H. Hamann, T. Hill, U. J. Katter, H. Schlienz, and H.-J. Freund, *Langmuir* **12,** 5512 (1996).
5. S. A. Goldman, G. V. Bruno, C. F. Polnaszek, and J. H. Freed, *J. Chem. Phys.* **56**(2), 716 (1972).
6. M. Farle, M. Zomack, and K. Baberschke, *Surf. Sci.* **160,** 205 (1985).
7. U. J. Katter, H. Schlienz, M. Beckendorf, and H.-J. Freund, *Ber. Bunsenges. Phys. Chem.* **97,** 340 (1993).
8. P. G. Barkley, J. P. Hornak, and J. H. Freed, *J. Chem. Phys.* **84,** 1886 (1986).
9. J. Pedereau, J. P. Biberian, and G. E. Rhead, *J. Phys. F: Metal Phys.* **4,** 798 (1974).
10. K. Marre and H. Neddermeyer, *Surf. Sci.* **287/288,** 995 (1993).

11. H. Hannemann, C. A. Ventrice, Jr., Th. Bertrams, A. Brodde, and H. Neddermeyer, *Phys. Status Solidi A* **146,** 289 (1994).

12. M. Beckendorf, Ph.D. thesis, Ruhr-Universität Bochum, 1995.

13. D. J. Schneider and J. H. Freed, *in* ''Spin Labeling: Theory and Applications'' (L. J. Berliner and J. Reuben, Eds.), Plenum Press, New York, 1989.

14. L. J. Libertini and O. H. Griffith, *J. Chem. Phys.* **53,** 1359 (1970).

15. R. G. Kostyanovskii and Kh. Khafizov, *Dokl. Akad. Nauk SSSR* **198,** 363 (Engl. 402) (1971).

16. P. A. Redhead, *Vacuum* **12,** 203 (1962).

17. D. Cappus, Ph.D. thesis, Ruhr-Universität Bochum, 1995.

18. M. J. Frisch, G. W. Trucks, M. Head-Gordon, P. M. W. Gill, M. W. Wang, J. B. Foresman, B. G. Johnson, H. B. Schlegel, M. A. Robb, E. S. Replogle, R. Gomperts, J. L. Andres, K., Raghavachari, J. S. Binkley, C. Gonzales, R. L. Martin, D. J. Fox, D. J. DeFrees, J. Baker, J. J. P. Stewart, and J. A. Pople, program package ''Gaussian,'' Revision A, Gaussian, Inc., Pittsburgh, Pennsylvania, 1992.

19. M. Zomack and K. Baberschke, *Surf. Sci.* **178,** 618 (1986).

20. G. P. Lozos and B. M. Hoffman, *J. Phys. Chem.* **78,** 2110 (1974).

21. A. H. Cohen and B. M. Hoffman, *J. Phys. Chem.* **78,** 1313 (1974).

22. M. Zomack, Ph.D. thesis, Freie Universität Berlin, 1987.

23. D. M. Eigler and S. Schultz, *Phys. Rev. Lett.* **54,** 1185 (1985).

24. M. T. Hutchings and E. J. Samuelsen, *Phys. Rev. B* **6,** 3447 (1972).

25. Y. Matsunaga and C. A. McDowell, *Can. J. Chem.* **38,** 724 (1960).

26. J. Yamauchi, T. Fujito E. Ando, H. Nishiguchi, and Y. Deguchi, *J. Phys. Soc. Jpn.* **25,** 1558 (1968).

27. J. Yamauchi, *Bull. Chem. Soc. Jpn.* **44,** 2301 (1971).

28. W. Duffy, Jr., D. L. Standburg, and J. F. Deck, *Phys. Rev.* **183,** 567 (1969).

29. J. A. Borchers, M. J. Carey, A. E. Berkowitz, R. W. Erwin, and C. F. Majkrzak, *J. Appl. Phys.* **73,** 6898 (1993).